A NUMERICAL MODEL ABOUT THE DYNAMIC BEHAVIOR OF A PRESSURE RELIEF VALVE

A. J. Ortega, arturo@simdut.com.br
B. N. Azevedo, bruno_n_azevedo@aluno.puc-rio.br
L. F. G. Pires, lpires@simdut.com.br
A. O. Nieckele, nieckele@puc-rio.br
L. F. A. Azevedo, Lfaa@puc-rio.br

Pipeline Thermo-Hydraulic Simulation Group – Mechanical Engineering Department – PUC/Rio
Rua Marques de São Vicente 225 – Gávea, CEP 22453-900, Rio de Janeiro, RJ, Brazil.

Abstract. *Pressure relief valve is one of the most important devices used on the security of pipelines, since it is responsible to guarantee the integrity of the installations. Generally, the response and behavior of a relief valve during its transient is unknown by users, who employ simplified and static analysis to design the pipeline, further, the information provided by manufactures is limited. In this work, a numerical dynamic model of a spring load pressure relief valve was developed using the principles of conservation of mass and momentum in combination with solid dynamics equation. The valve discharge coefficient was numerically determined by employing a simplified two-dimensional model with FLUENT. The dynamic characteristics of the valve were examined with regard to the pressure set point, disc lift and spring parameters, during the transient discharge flow.*

Keywords*: Pressure relief valve, dynamic characteristics, transient discharge flow.*

1. INTRODUCTION

Relief and safety valves are fundamental equipments for oil and gas pipelines and load/unload terminals. The installation integrity and workers safety depend on the appropriate design and performance of these equipments. In spite of the importance of relief valves, there is lack of information about the dynamic behavior of these equipments. Thus, users are forced to work using valve characteristics supplied only by manufactures. Further, the information supplied by manufactures is generally restricted to situations of maximum pressure relief flow. The full dynamic behavior of the relief valves during their opening stage, which is fundamental for analysis of transients during their actuation, is usually not available.

Due to the importance of relief valves, a few works about its dynamic behavior has been published. Catalani (1984) performed a dynamic stability analysis of a relief valve and identified the effects of its components on its stability. The undesired phenomenon named *chatter* (abrupt oscillations of the disc) was studied by MacLeod (1985) who modeled, using differential equations, the dynamic of a relief valve and identified the conditions to avoid it. In 1991 Shing made a study about the dynamic and static characteristics of a two stage pilot relief valve and determined the governing parameters of the valve response which could be improved. The dynamic of a direct operated relief valve with directional damping was studied by Dasgupta et al (2001) using the *bondgraph* technique. Maiti et al (2002) studied the dynamic characteristics of a two-stage pressure relief valve with proportional solenoid control of its pilot stage. According to their results, the overall dynamic behavior is dominated by the solenoid characteristic relating force to applied voltage. Boccardi et al (2004) analyzed experimentally the water/vapor two phase flow through a relief valve. A new correlation for the discharge coefficient was developed, by comparing the experimental data with the solution of the flow based on a homogeneous model.

The objective of this work is to simulate the dynamic behavior of a direct acting spring loaded pressure relief valve (*PRV*) during its actuation. The identification of its governing parameters will allow the extension of the analysis to more general and real cases.

2. MATHEMATICAL MODEL

Although the dynamic behavior of a *PRV* is strongly influenced by its geometric configuration and dimensions, a simplified geometry, as shown in Fig. 1, was considered to the development of a mathematical model. The simplified system is composed of a spring, a cap or disc and a input flow pipe (valve wall). For the flow analysis through the *PRV*, the fluid was considered as incompressible and isothermal. Due to the cylindrical shape of the geometry, the flow was considered axi-symmetric.

2.1. Dynamic characteristic

The *PRV* starts opening when the operation pressure P_a exceeds the set point pressure P_{sp}. During the disc displacement, the Newton's second law can be applied to the system illustrated in Fig. 2, resulting in the spring-disc dynamic system equation, Eq. (1).

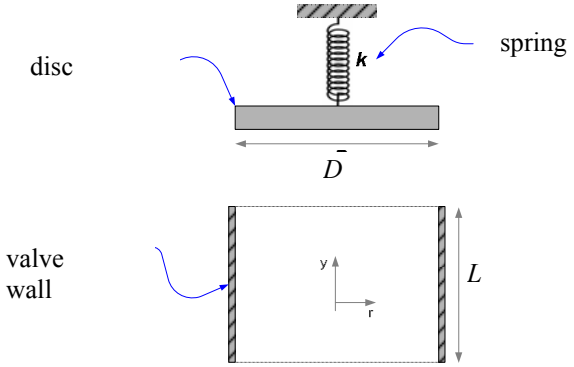

Figure 1 – *PRV* simplified system

$$F_f - k(Y_D + Y_o) - c\frac{dY_D}{dt} - m_D g - P_o A = m_D \frac{d^2 Y_D}{dt^2}, \tag{1}$$

where F_f is the force applied by fluid to disc, k is the spring constant, Y_D is the disc displacement, Y_o is the spring initial deformation, c is the spring viscous damping coefficient, m_D is the disc mass, g is the gravity acceleration, P_o is the external pressure (atmospheric pressure) and A is the cross section of the little pipe / disc area.

Applying the principle of conservation of linear momentum in the y direction, to control volume inside the *PRV* illustrated in Fig. 3, neglecting the time y momentum variation inside the control volume, since it can be considered small in relation to the others quantities, results in

$$\sum F_y = \frac{\partial}{\partial t}\int_{CV} u\,\rho\,d\forall + \int_{CS} u\,\rho\,\vec{u}\bullet d\vec{A} \;\Rightarrow -\rho g A(L + Y_D) - F_f + P_a A = -u_e \rho u_e A, \tag{2}$$

where ρ is the fluid density, L is the length of the valve wall, F_f is the reaction applied by the disc to fluid, u_e is the average velocity coming into the control volume and P_a is the operation pressure or the *PRV* input pressure.

Combining the spring-disc dynamic equation, Eq. (1), with the fluid conservation equations, Eqs. (2) and (3), the following expression is obtained

$$0 = m_D \frac{d^2 Y_D}{dt^2} + c\frac{dY_D}{dt} + (k + \rho g A)Y_D + kY_o + \rho g AL + m_D g - (P_a - P_o)A - Q^2\frac{\rho}{A}, \tag{3}$$

where $Q = \rho u_e A$ is the average flow rate coming into the control volume.

The initial spring displacement Y_o can be determined as a function of the set point pressure P_{sp} to open the relief valve, by applying Eq. (3) to the instant immediately before the valve opening, i.e., $Y_D = 0$ and Q=0, P_a=P_{sp}.

$$Y_o = \frac{1}{k}\left[(P_{sp} - P_o)A - \rho g A L - m_D g\right]. \tag{4}$$

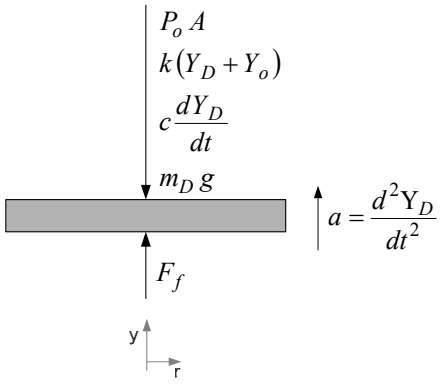

Figure 2 – The disc free body diagram during its displacement

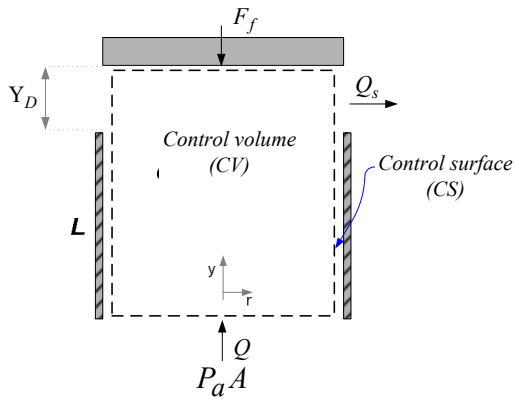

Figure 3 – Control volume inside of the *PRV* during its actuation

Equating (3) can be simplified with Eq. (4) as

$$0 = m_D \frac{d^2 Y_D}{dt^2} + c \frac{dY_D}{dt} + (k + \rho g A) Y_D - (P_a - P_{sp}) A - Q^2 \frac{\rho}{A}. \tag{5}$$

Applying the principle of mass conservation into the *PRV* control volume during its actuation, Fig. 3, the average flow rate that exits from the control volume Q_s can be related with the inflow rate Q and the disc displacement Y_D as

$$0 = \frac{\partial}{\partial t} \int_{CV} \rho \, d\forall + \int_{SS} \rho \, \vec{u} \bullet d\vec{A} \quad \Rightarrow \quad 0 = A \frac{dY_D}{dt} - Q + Q_S, \tag{6}$$

Further, the valve outflow rate Q_s can be defined by the valve equation as

$$Q_S = C_d A \sqrt{2 \frac{(P_a - P_o)}{\rho}}, \tag{7}$$

where C_d is the valve coefficient and A is a reference area, in this work it was considered as the disc area.

Finally, the equation that governs the dynamic behavior of the *PRV* during its actuation can be obtained by combining Eqs. (7), (6) and (5) as

$$\begin{aligned} 0 = {} & m_D \frac{d^2 Y_D}{dt^2} + \left(c - 2C_d A \sqrt{2\rho(P_a - P_o)}\right) \frac{dY_D}{dt} + \\ & + (k + \rho g A) Y_D - (P_a - P_{sp}) A - \left(\frac{dY_D}{dt}\right)^2 \rho A - 2C_d{}^2 A (P_a - P_o) \end{aligned} \tag{8}$$

2.2 Initial and Boundary Conditions

Initially it is considered that the *PRV* is closed (Y_D=0 and $d\,Y_D/d\,t = 0$). The flow through the valve begins when the operation pressure P_a exceed the set point pressure P_{sp}. When the disc reaches its maximum position $Y_{D\mathbf{max}}$, there is no more displacement, and the disc wall reaction R_D for this situation can be obtained from Eq. (1) as

$$-\rho g A (L + Y_{D\mathbf{max}}) - R_D + P_a A = -Q^2 \frac{\rho}{A}, \tag{9}$$

and the inflow and outflow volumetric flow rate through the valve is the same, Q=Q_s. The flow rate can be calculated using the Eq. (7). A similar situation occurs when the disc displacement reaches its minimum position, $Y_{D\mathbf{min}}$=0, and the *PRV* is closed.

2.3. Dimensionless Parameters

The mathematical model, described by Eq. (8), can be normalized considering it as an oscillation-damping system, with $Y_D{}^* = Y_D/D$, $t^* = t\,\nu/D^2$ and $P^* = P/(\rho\nu^2/A)$ where ν is the cinematic viscosity as

$$\begin{aligned} 0 = {} & \frac{d^2 Y_D{}^*}{dt^{*2}} + 2\xi^* \omega_o{}^* \left(1 - \sqrt{2\pi} C_d \frac{1}{C^*} \sqrt{P_a{}^* - P_o{}^*}\right) \frac{dY_D{}^*}{dt^*} + \\ & + \omega_o{}^{*2} \left(1 + \psi^*\right) Y_D{}^* - \left(P_a{}^* - P_{sp}{}^*\right) \frac{1}{m_D{}^*} - \frac{\pi}{4} \left(\frac{dY_D{}^*}{dt^*}\right)^2 \frac{1}{m_D{}^*} - 2C_d{}^2 \frac{1}{m_D{}^*} \left(P_a{}^* - P_o{}^*\right) \end{aligned}, \tag{10}$$

The resulting dimensionless parameters that govern the valve behavior are listed in Table 1.

3. NUMERICAL METHOD

Equation (10) was solved numerically using a fourth-order *Runge-Kutta* method. The numerical algorithm was implemented using *Fortran*.

Table 1 - Dimensionless Parameters

Parameters	
$\omega_o^* = \omega_o \frac{D^2}{\upsilon}$	Dimensionless natural frequency, $\omega_o = \sqrt{\frac{k}{m_D}}$
$\xi^* = \frac{c}{2\sqrt{k\, m_D}}$	Damping ratio.
$\psi^* = \frac{\rho\, g\, A}{k}$	Relation between the fluid weight per length unit and the spring constant.
$m_D^* = \frac{m_D}{\rho\, D^3}$	Dimensionless disc mass.
$C^* = \frac{c}{\upsilon\, \rho\, D}$	Dimensionless viscous damping coefficient.
C_d	Valve coefficient.
$Y_{D\mathbf{max}}{}^* = \frac{Y_{D\mathbf{ma}}}{D}$	Dimensionless disc maximum displacement.

Among the several parameters listed on Table 1, the valve coefficient C_d is the critical parameter to be specified. It depends on the flow distribution inside the valve. Usually, it is determined experimentally, based on steady state flow with different valve openings. At the present work, the discharge coefficient was determined numerically, considering a steady state regime for different valve openings, as it is done experimentally.

3.1. Discharge Coefficient

The valve coefficient, C_d, was determined from the flow field inside the simplified valve, illustrated in Fig. 1, employing the software FLUENT, with the following dimensions: L = 0.2 m, D = 0.1m and Y_{Dmax} = 0.1 m. The valve was considered axi-symmetric, therefore, several 2D turbulent steady state flow were obtained, for different valve openings, through the solution of the Reynolds-averaged mass and momentum equations (RANS) given by

$$\frac{\partial\, \overline{u_j}}{\partial\, x_j} = 0 \tag{11}$$

$$\frac{\partial}{\partial x_j}\left(\rho\, \overline{u_i}\, \overline{u_j}\right) = -\frac{\partial\, p}{\partial x_i} + \frac{\partial}{\partial x_j}\left[(\mu + \mu_t)\left(\frac{\partial \overline{u_i}}{\partial x_j} + \frac{\partial \overline{u_i}}{\partial x_j}\right)\right] \tag{12}$$

where $\overline{u_j}$ is the time average velocity, μ and μ_t are the absolute and turbulent viscosity, and P is the pressure. The turbulent viscosity was determined with the κ–ω SST model (Menter, 1994), which was developed to blends the effectively robust and accurate formulation of the standard κ–ω model in the near-wall region with the free-stream independence of the κ–ε model in the far field. The blending is designed to be one in the near-wall region, which activates the standard κ–ω model, and zero away from the surface, which activates the transformed κ–ε model. The turbulent eddy viscosity μ_t is defined as

$$\mu_t = \rho\, \frac{k}{\omega\, \varepsilon} \tag{13}$$

where ω is the specific dissipation, and ξ is the blending term. There is also a cross-diffusion term D_ω included to the ω equation. The model requires the solution of two conservation equations, one is the standard κ equation, and the other is specific dissipation ω equation. These equations are given as

$$\frac{\partial}{\partial\, x_j}\left(\rho\, \overline{u_i}\ \kappa\right) = \frac{\partial}{\partial x_j}\left[\Gamma_\kappa\, \frac{\partial\, \kappa}{\partial\, x_j}\right] + G_\kappa - Y_\kappa + S_\kappa \quad ; \quad \frac{\partial}{\partial\, x_j}\left(\rho\, \overline{u_j}\ \omega\right) = \frac{\partial}{\partial\, x_j}\left[\Gamma_\omega\, \frac{\partial \omega}{\partial\, x_j}\right] + G_\omega - Y_\omega + D_\omega + S_\omega \tag{14}$$

where G_κ represents the production of turbulent kinetic energy due to mean gradients, while G_ω is the production of ω. $\Gamma_\kappa = \mu+\mu_t/\sigma_\kappa$ and $\Gamma_\omega = \mu+\mu_t/\sigma_\omega$ are the effective diffusivity of κ and ω, where σ_κ and σ_ω are the turbulent Prandtl numbers for of κ and ω, respectively. Y_κ and Y_ω are the destruction of κ and ω, due to turbulence. The model is presented in detail in *FLUENT,* v6.3 (2008).

The operating pressure P_a = 2 atm was set at the inlet and the discharge pressure P_o was set as 1 atm. Water was selected was the working fluid (ρ = 1000 kg/m^3 and μ= 10^{-3} Pa-s). Figure 4 illustrates the streamline distribution for a particular opening, where the bending of the flow toward the valve exit can be clearly seen.

From the converged flow field, the valve coefficient C_d was calculated using Eq. (7). Figure 5 presents the valve coefficient C_d as a function of the different opening, normalized by the maximum aperture $Y_{D\mathbf{max}}$ (Y'_D=Y_D/$Y_{D\mathbf{max}}$). At the same figure, a third order polynomial adjusted to fit the data was plotted. This polynomial was included in Eq. (10) to determine the dynamic of the valve aperture.

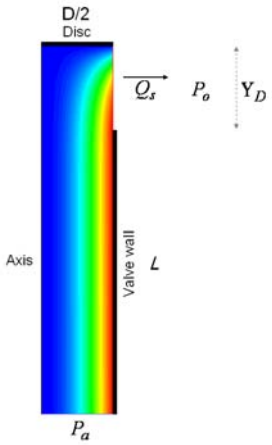

Figure 4 – Streamlines into the *PRV* geometry used for C_d calculation, Y_D = 0.040 m

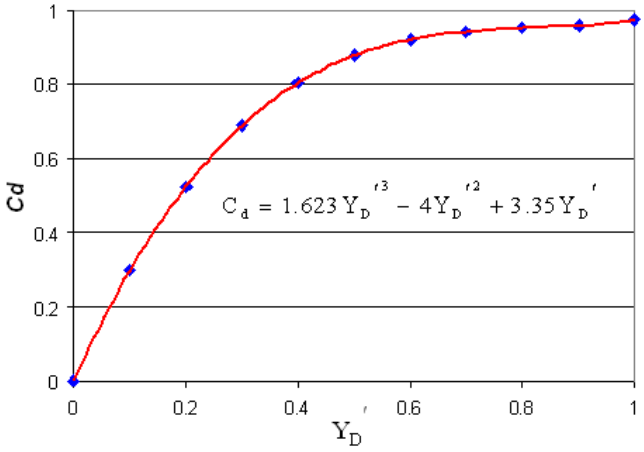

Figure 5 – Valve coefficient calculated numerically

4. RESULTS

To validate the developed computational code, several test cases were performed. The pressure set point and operational pressure were defined as P_{sp} = 2 kgf/cm^2 and P_a = 3 kgf/cm^2. The spring dimensional parameters were specified as: k = 4kgf/mm, c = 31 kgf-s/m, m_D = 200 g. For this situation the initial spring displacement Y_o is 18.5 mm.

Figure 6 shows the *PRV* disc displacement along the time. On the beginning of the *PRV* opening the disc has reached its maximum displacement, followed by a strong oscillation, which was damped as time increased, reaching an equilibrium displacement of 90.4 mm, after 0.25s. The Figure 7 shows the time variation of the inlet and outlet flow rate through the *PRV*. Initially, there is a great difference among the two quantities, due to the increase of the valve volume. As the disc stabilizes, there is no more volume change, equating the inlet and outlet flow rate to 532.3 m^3/h after 0.25 s.

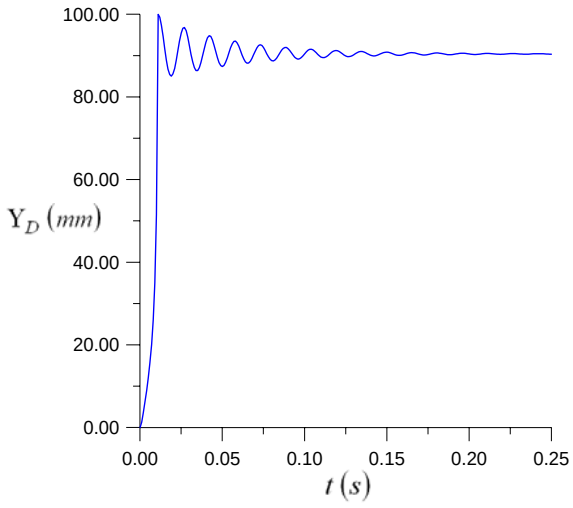

Figure 6 – *PRV* disc displacement through the time

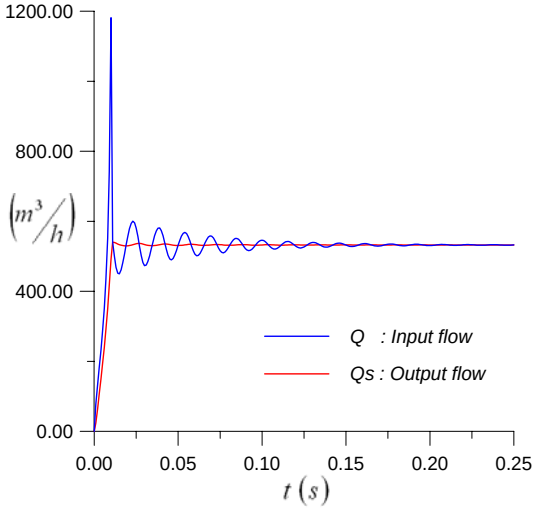

Figure 7 – *PRV* input and output flow rate through the time

In other to analyze the sensibility of the disc displacement to its several parameters, additional tests were performed. The influence of viscous damping coefficient *c* on the disc displacement is illustrated at Fig. 8. As expected, it can be seen that for large *c* the initial perturbations are smaller and the disc equilibrium occurs more rapidly. In the equilibrium stage, the three cases reached the same disc displacement equal to 90.4 mm.

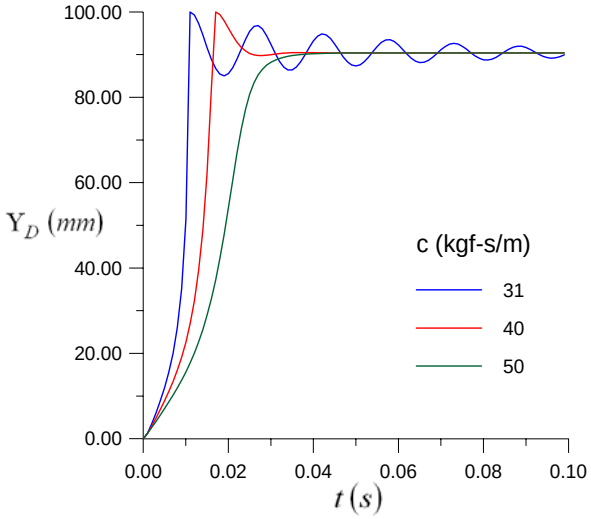

Figure 8 – Influence of the viscous damping coefficient in the *PRV* disc displacement

The influence of the spring coefficient *k* is shown in Fig. 9. It can be observed that higher *k* values lead to higher values of disc reaction force against fluid, causing larger amplitude oscillations in the first instants of the *PRV* actuation. However, as a result of the greater resistance to disc displacement, it reaches equilibrium more rapidly, in a position with smaller displacement. Smaller *k* values imply less resistance to disc displacement, leading to the total opening of the *PRV* in the first instants of its actuation.

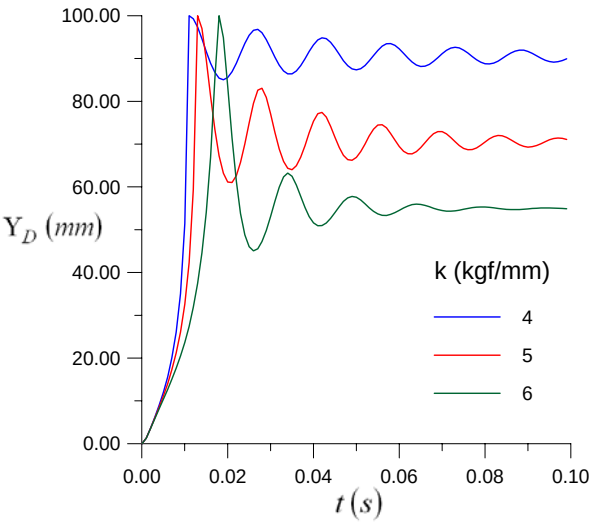

Figure 9 – Influence of the spring constant in the *PRV* disc displacement

Figure 10 shows the influence of the disc mass in the valve aperture. Note that, by increasing the disc mass, the maximum displacement and the equilibrium are reached more slowly. The equilibrium disc displacement was equal to 90.4 mm in the three cases. Increasing the disc mass reduces the natural spring frequency ω_o, leading to longer waves with smaller frequency, increasing the time required to reach equilibrium.

The influence in the disc displacement due to the operation pressure at the inlet of the *PRV* is shown in Fig. 11. It can be seen that smaller operation pressure values, lead to smaller disc oscillations. The disc equilibrium is more rapidly reached, since the disc equilibrium displacement is proportional to its external force caused by the operation pressure.

Figures 12 and 13 illustrate the influence of the maximum displacement of the *PRV* disc in its operation. For these tests, the polynomial curve for $C_d \times Y'_D$ was adjusted to the new maximum displacement. Three different maximum displacements were considered: 25 mm, 50 mm and 100 mm.

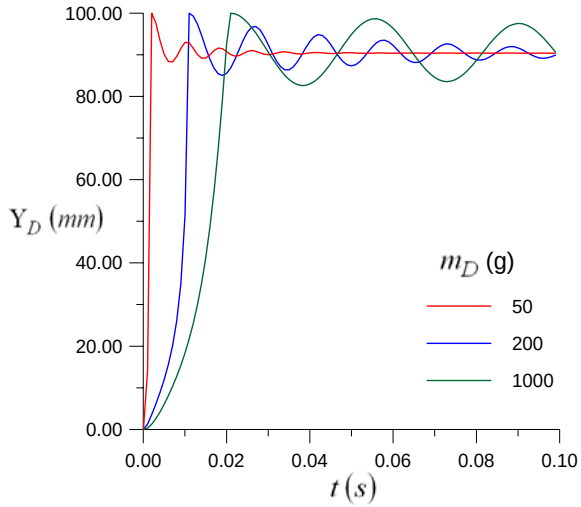

Figure 10 – Influence of the disc mass in the *PRV* disc displacement

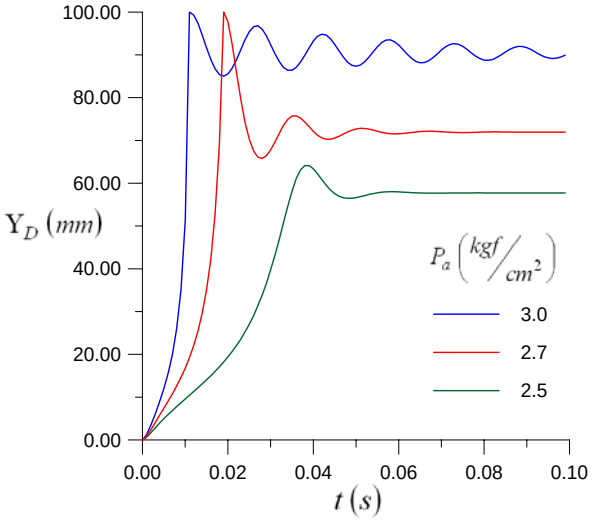

Figure 11 – Influence of the operation pressure in the *PRV* disc displacement

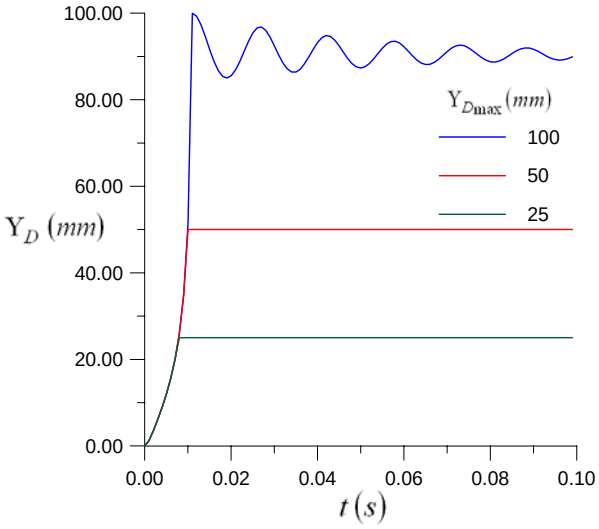

Figure 12 – Influence of the disc maximum displacement in the *PRV* disc equilibrium

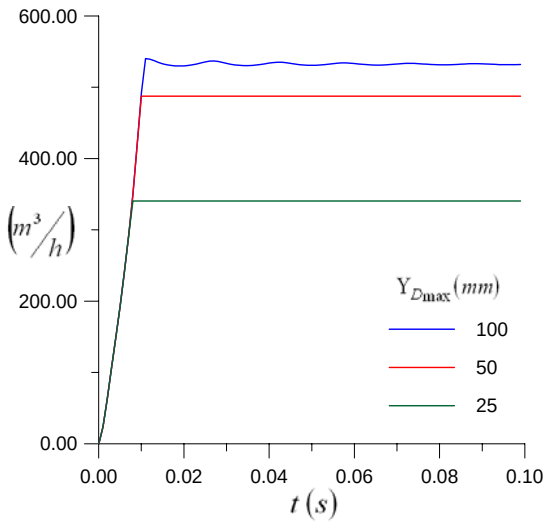

Figure 13 – Influence of the disc maximum displacement in the *PRV* flow equilibrium

Figure 12 shows the influence of the maximum displacement in the valve dynamic aperture, while Fig. 13 shows the flow rate through the valve. Since the driving force is high, the disc rapidly reaches its maximum position, and no oscillation is observed, and as expected, smaller flow rate is obtained. However, it can be seen in Fig. 13 that although the maximum disc displacement was reduced in 50%, there was a reduction of only 27% of the flow rate.

5. FINAL REMARKS

The present work has derived a mathematical model for a direct acting spring loaded pressure relief valve. The developed mathematical model predicts the disc behavior and the input – output flow rate of the relief valve during its transient (dynamic characteristics) and equilibrium state. Although a simplified geometry was considered, the methodology can be applied to more complex geometries.

A sensibility analysis was performed, by analyzing the influence of the several governing parameters in the valve disc displacement, and reasonable results were obtained.

As a next step to the present analysis, two fronts are being pursued. In the first one, an experimental apparatus is being built to allow comparison with the model predictions. The second front consists of improving the numerical determination of the valve coefficient C_d, by employing a 2D transient analysis of the flow inside the valve.

6. ACKNOWLEDGEMENTS

The authors thank FINEP for supporting the development of this work.

7. REFERENCES

API RP 520, 2000, “Sizing, Selection and Installation of Pressure-Relieving Devices in Refineries”, Seventh edition, American Petroleum Institute.

Boccardi, G., Bubbico, R., Celata, G.P. and Mazzarotta, B., 2005, “Two-Phase Flow Through Pressure Safety Valves – Experimental Investigation and Model Prediction“, Chemical Engineering Science Vol. 60, pp. 5284-5293.

Catalini, L., 1984, “Dynamic stability analysis of spring loaded safety valves – Elements for improved valves performance through assistance devices”. Conference on Structural Mechanical in Reactors, August 22-26.

Dasgupta, K. and Karmakar, R., 2002, “Modelling and dynamic of single-stage pressure relief valve with directional damping”, Simulation Modelling Practice, Vol. 10, pp. 51-57.

Fox, R.W.and McDonald, A.T., 1998, “Introduction of Fluid Mechanics”, John Wiley & Sons Inc.

Fluent Users Guide, 2008, Fluent Inc.

Macleod, G., 1985, “Safety valve dynamic instability: an analysis of chatter”, ASME Journal of Pressure Vessel Technology, Vol. 107, pp. 172-177.

Maiti, R., Saha, R. and Watton, J., 2002, “The static and dynamic characteristics of a pressure relief valve with a proportional solenoid-controlled pilot stage”, Proc Instn Mech Engrs, Vol. 216, Part I, pp 143-156.

Menter, F. R., Kuntz, M. and Langtry, R., 2003, “Ten Years of Industrial Experience with the SST Turbulence Model”, Proceedings of the 4th International Symposium on Turbulence, Heat and Mass Transfer, pp. 625-632.

Potter, M.C. and Wiggert, D.C., 1997, “Mechanics of Fluids”, Second Edition, Prentice Hall Inc.

Shin, Y.C., 1991, “Static and Dynamic Characteristics of a Two Stage Pilot Relief Valve”, Journal of Dynamic Systems, Measurement, and Control, Vol. 113, pp. 280-288.

Wylie, E.B. and Streeter V.L., 1993, “Fluid Transients in Systems”, Prentice Hall Inc.

Zappe, R.W., 1998, “Valve Selection Handbook”, Fourth Edition, Goulf Professional Publishing.

8. RESPONSIBILITY NOTICE

The authors are the only responsible for the printed material included in this paper.